

Plasma Sci. Technol. **19** (2017) 045301 (8pp) https://doi.org/10.1088/2058-6272/aa58db

Analysis of incoherent scatter during ionospheric heating near the fifth electron gyrofrequency

Jun WU (吴军)[1], Jian WU (吴健), Haisheng ZHAO (赵海生) and Zhengwen XU (许正文)

National Key Laboratory of Electromagnetic Environment, China Research Institute of Radiowave Propagation, Beijing 102206, People's Republic of China

E-mail: wujun1969@163.com

Received 31 May 2016, revised 8 January 2017
Accepted for publication 10 January 2017
Published 9 March 2017

Abstract

The observation of ultra-high frequency radar during an ionospheric heating experiment carried out at Tromsø site of European Incoherent Scatter Scientific Association, Norway, is analyzed. When pump is operating slightly above the fifth electron gyrofrequency, some strong enhancements in radar echo and electron density occur in a wide altitude range and are in sync with the shifting and spread of plasma line around the reflection altitude, which may be due to the focusing or collimating of radar wave by irregularities. While some strong enhancements in electron density and radar echo around the reflection altitude do not correspond to the true increase in electron density, but due to the enhanced ion acoustic wave by parametric decay instability and oscillation two stream instability. In addition, the different heating rates and cooling rates at the pump frequencies below, around and above fifth gyrofrequency respectively result in the dependence of the enhancements in electron temperature on the pump frequency.

Keywords: ionospheric heating, incoherent scatter, electron temperature, electron density

(Some figures may appear in colour only in the online journal)

1. Introduction

High-power ground-based high-frequency radio below the critical frequency of the ionosphere has been used in so-called ionospheric heating experiments since 1970. A wide range of phenomena were presented, the most common of which were the enhancement in electron temperature and the perturbations of electron density in either enhancement or reduction. Gordon *et al* [1, 2] reported the effect of ionospheric heating on the vertical electron temperature profile above Arecibo, which showed that the stronger pump power, the more significant the mean enhancement in electron temperature, and the enhancement in electron temperature usually took place for pump in O mode. Combining with strong heat conduction along the geomagnetic field, Newman *et al* [3] showed that the dramatically large temperature enhancement was attributable primarily to the low cooling rate of plasma, rather than the high heating rate. Duncan *et al* [4] presented some observations of density depletions exceeding 50% with electron temperature increased by a factor of 3 to 4 in the depletion region, extending hundreds of kilometers along the geomagnetic field. These density depletions were thermally driven. At EISCAT (European Incoherent Scatter Scientific Association), during O-mode heating at full power, the electron temperature increased up to 55%, whereas the measurements of electron density revealed both enhancements and reductions in the vicinity of the reflection altitude of pump [5].

Apart from Ohmic heating, the wave–particle interaction near the resonance region play an important role in electron temperature enhancement and electron density reduction. Utlaut and Violette [6] reported for the first time that anomalous absorption was visible on ionograms from slightly below the pump frequency up to the F region critical

[1] Author to whom any correspondence should be addressed.

frequency. For this reason, the anomalous absorption was originally termed as wide band absorption. Mantas *et al* [7] found that the induced enhancement in electron temperature by pump spread over a broader altitude range, for which heat conduction was responsible, and that about half the heating was caused by anomalous absorption and half by derivative absorption. However, those later observations provided some evidences that anomalous electron heating in the presence of small scale field aligned irregularities dominated over collision heating at high latitude [8]. Gurevich *et al* [9] established a nonlinear theory determining the conditions for the existence and structure of the stationary small scale irregularities induced by ionospheric heating, and predicted a strong enhancement in electron temperature inside the small scale irregularities and considerable change of the depth of the irregularities. Furthermore, Gurevich *et al* [10] constructed a nonlinear theory of anomalous absorption of a powerful pump on small scale irregularities. With regard to the problem of the nonlinear structuring of the modified ionosphere due to the self focusing of a pump on the bunches of small scale irregularities, two main conditions of self-focusing, namely, propagation of pump along the magnetic field for effective excitation of small scale irregularity and trapping of pump by large scale irregularities [11].

It has been found that those enhancements in electron temperature also exhibit a dependence on the difference between the pump frequency and a harmonic of the electron gyrofrequency. Mjolhus [12] predicted that the effect of ionospheric heating should be suppressed when the pump frequency was slightly below a harmonic of the electron gyrofrequency. Moreover, the peculiarities of the absorption of pump near the third electron gyrofrequency were investigated. Some experiments were carried out and have confirmed the above theories and predications. Measurements of anomalous absorption of pump and enhancement in electron temperature all exhibited broad minima as the heater frequency approached the third electron gyrofrequency. The results suggested that pump could not excite the small scale field aligned irregularities at pump frequencies in the vicinity of the third electron gyrofrequency [13]. Likewise, the results given by Robinson *et al* [8] indicated that there were strong minima in the responses of both anomalous absorption and electron temperature in the vicinity of the third and fourth electron gyrofrequency, which provided the evidence that anomalous electron heating in the presence of small scale field aligned irregularities dominated over collision heating at high latitudes. Experimental results of resonant high frequency scattering from small scale field aligned irregularities excited by pump transmitted by the Sura radio facility in Russia also showed a minimum in the scattered signal intensity when the pump frequency was near the fourth electron gyrofrequency and a significant broadening of the frequency spectrum of the scattered signal for pump frequencies above the fourth electron gyrofrequency [14]. Borisova *et al* [15, 16] presented that the coexistence of the thermal parametric instability and PDI (parametric decay instability) in the vicinity of the fourth gyroresonance harmonic, an increase in the electron number density by 40%–50% and a weak suppression of artificial ionospheric irregularities with the transverse scales of 7.5–9.0 m during heating at a frequency near the fifth electron gyroharmonic. Wu *et al* [17] presented the electron temperature enhancement variation near the reflection region and the electron density enhancement extended a wide range for pumping near electron gyrofrequency, where the later was actually not a true enhancement, but it may be due to some other mechanism.

In this paper, the further results from the EISCAT UHF incoherent scatter radar will be presented for an experiment at EISCAT near the fifth electron gyrofrequency.

2. Experiment setup

The EISCAT heater [18] is located near Tromsø, Norway (69.58°N, 19.21°E, magnetic dip angle $I = 78°$). The 12 transmitters can generate up to ~1.2 MW of continuous wave power in the frequency range from 3.85 to 8 MHz. There are three antenna arrays that cover the frequency ranges of 3.85–5.65 MHz and 5.5–8 MHz, with a gain of ~24 dB (dependent on frequency), and can produce a beam width of 14.5° and a maximum effective radiated power of ~360 MW. The principal diagnostic, EISCAT UHF radar [19] located near the EISCAT heater, is an ISR (incoherent scatter radar) operating at 930 MHz. The antenna is a 32 m parabolic dish with a beam width of ~0.5° at half-maximum power. It is fully steerable in azimuth and elevation.

A detailed description of the experimental arrangement and the ionosphere background has been given by Wu *et al* [17]. In short, the experiment involved the O mode pump operated at frequencies near the fifth gyrofrequency $5\Omega_{ce}$ as shown in the bottom panel of those following figures and with the beam directed field-aligned (actually 12° south of the zenith), EISCAT UHF radar being pointed field-aligned and running 'beata' modulation mode with a undecoded ~96 km range resolution and a decoded ~3 km range resolution, and the relatively inactive ionospheric and geomagnetic condition, where Ω_{ce} is the local electron gyrofrequency at the altitude of ~200 km with a value of ~1.366 MHz in Tromsø.

3. Observations and analysis

3.1. ISR backscatter

To measure the effect of pump at individual frequency, an integrated time of 10 s will be used in the following data analysis. Figure 1 shows the ratios of the undecoded UHF radar echo P to the undisturbed values of P_0 as a function of heating cycles within the altitude range from 76.6 to 720 km, where P_0 is the median of UHF radar echo taken from the observations in the final 5 min of the last cycle (14:25 UT–14:30 UT). In order to facilitate the following description and discussion, it is necessary to divide the pump frequency band of [6.7 MHz, 7 MHz] into three bands, namely, the high frequency band (HB), the gyrofrequency band (GB) and the low frequency band (LB), for instance HB for (6.857 009 MHz,

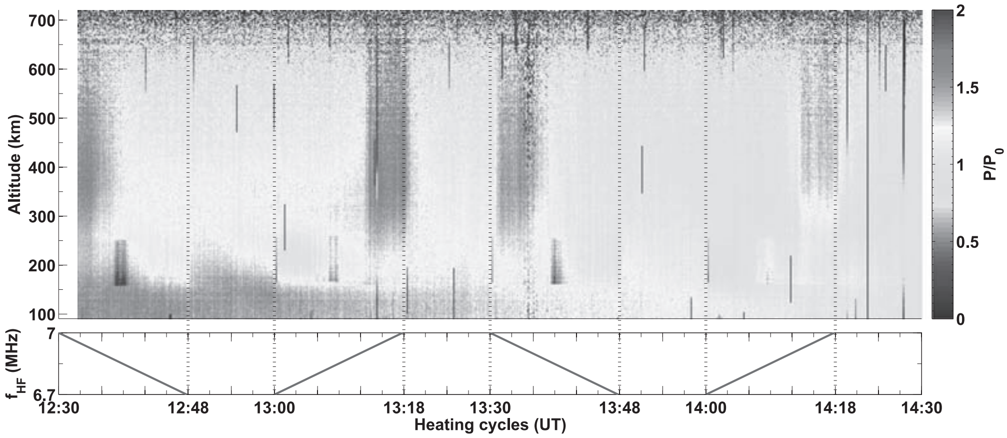

Figure 1. The undecoded UHF radar echo with a height resolution of 94 km.

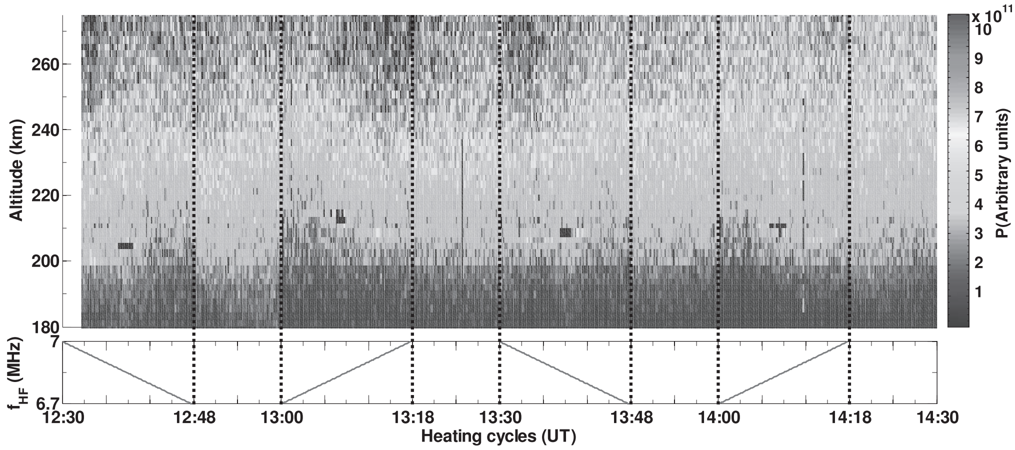

Figure 2. The decoded UHF radar echo with a height resolution of ~2.4 km.

7 MHz], GB for [6.84 299 MHz, 6.857 009 MHz] and LB for [6.7 MHz, 6.84 299 MHz) respectively in the third cycle, where '( )' means the open interval. Indeed, due to the perturbation of the geomagnetic field, the above division in each cycle should be slightly different from each other.

In figure 1, there are two types of strong enhancements in P/P_0, one of which occurs over the altitude range from ~155 to ~250 km in the GB and is at level of ~1.6 to ~2, and the second one of which appears to be independent of altitude and extends from ~230 to ~700 km and takes place in the HHB and develops up to $P/P_0 \approx \sim 1.5$, where HHB denotes those higher frequencies of (~6.93–7 MHz] in the HB. In the third cycle, the enhancement does not appear immediately after pump is switched on, but 30 s later. In the second and fourth cycles, however, the enhancements decay to the undisturbed level within 30 s.

On the other hand, some decreases in P/P_0 of up to ~0.85 take place in the LB and within the altitude range of from ~155 to ~250 km in all of cycles, and become weaker at those pump frequencies f_{HF} being closer to GB. Additionally, they appear immediately after pump is switched on as seen in the second and fourth cycles, and disappear immediately after pump is switched off as shown in the first and third cycles.

The decoded power profile of radar echo with a height resolution of ~2.4 km over the altitude range of 180–276.8 km is presented in figure 2 to determine the reflection altitude of the pump more clearly. Due to the Bragg condition, a radar with frequency f_{r} in monostatic operation detects the propagating Langmuir waves and ion acoustic waves enhanced by the pump at the altitude [20]

$$z = z_0 - 12\frac{v_{\mathrm{e}}^2 f_{\mathrm{r}}^2}{c^2 f_{\mathrm{HF}}^2}H, \quad (1)$$

where z_0 denotes the reflection altitude of pump, v_{e} thermal electron velocity, c the velocity of light and f_{HF} the pump frequency. Considering the operating frequency of EISCAT UHF radar $f_{\mathrm{r}} = 930$ MHz, the pump frequency $f_{\mathrm{HF}} = 7$ MHz, the electron temperature $T_{\mathrm{e}} = 2000$ K and H the scaled height with a reasonable value of ≈50 km at the altitude of 200 km, then formula (1) can be expressed as $z = z_0 - 7.4$ km, with respect to the experiment in this paper, the reflection altitude of the pump should be within the altitude range of ~207.4 to ~222.4 km.

3.2. ISR spectrum

As some examples, the ion lines within the interval of −20 – 20 kHz at altitudes of 203.7 km, 206.63 km,

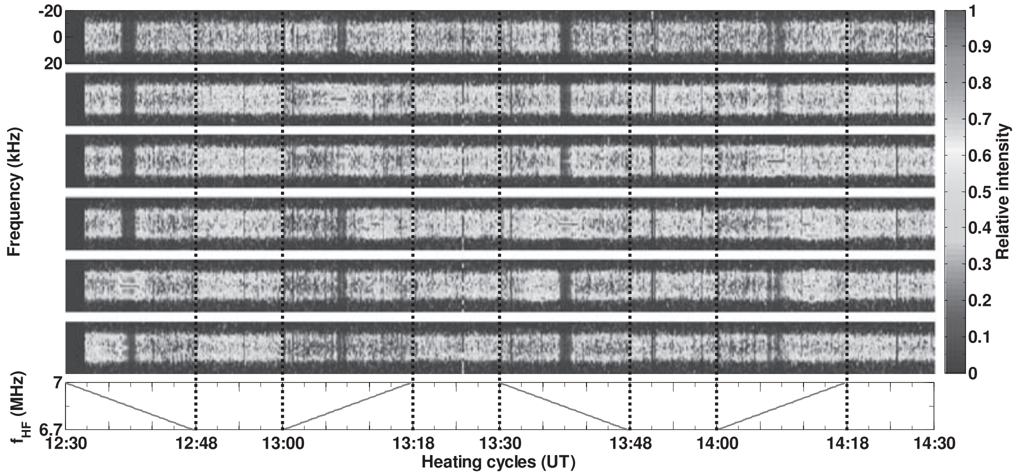

Figure 3. The ion lines from –20 to 20 kHz versus heating cycles, where they are placed from the top panel to the sixth panel for the altitudes of 203.7 km, 206.63 km, 209.58 km, 212.51 km, 215.43 km and 344.68 km respectively.

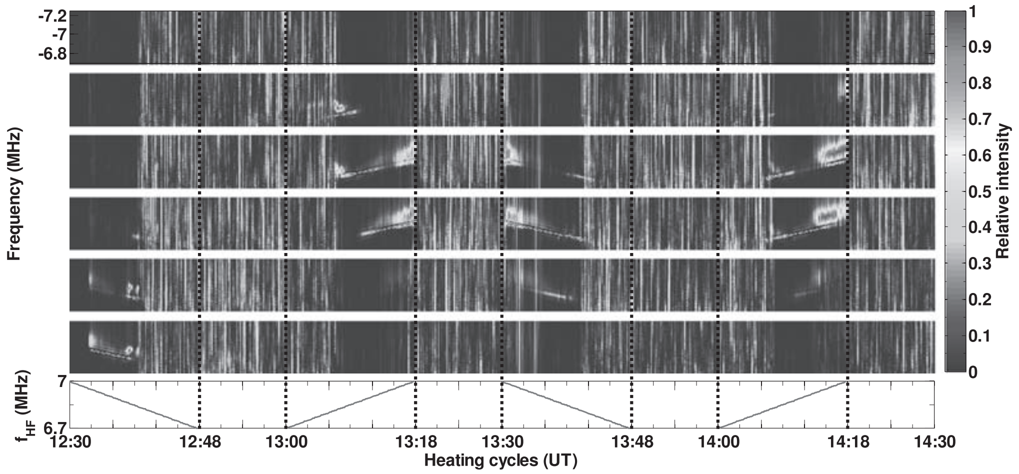

Figure 4. The downshifted plasma line from −6.7 to −7.25 MHz versus heating cycles, where they are placed from the top panel to the sixth panel for the altitudes of 198.52 km, 201.45 km, 204.39 km, 207.32 km and 339.48 km respectively.

209.57 km, 212.5 km, 215.43 km and 344.68 km are given in figure 3 respectively. When the pump sweeps in the GB, there are some 'breakdowns' of ion line spectrum, which indicate that the normalization value of ion line is suddenly decreased. Here it is necessary to point out that those 'breakdowns' are caused by the individual normalization of ion line at particular moment and does not imply the real decrease in ion line and any unusual response.

At the altitude of 344.68 km, the ion line shows some distinctive enhancements when heating in the HHB, which are corresponding to the enhancements in P/P_0 extending over a wide altitude range. In the HB and GB, The most prominent features are the significant 'spikes' in the center of ion line spectrum and the significant 'shoulders' at ∼9.5 kHz around the reflection altitude, which are the confirmation of PDI and OTSI (oscillation two stream instability) respectively [20, 21]. On the other hand, there are some declines in ion line spectrum in the LB around the reflection altitude, which are associated obviously with those declines in P in the LB.

The previous observations at EISCAT showed that the altitude of the ion line was about ∼3 to ∼5 km higher than the altitude of the plasma line [20, 21]. Considering the above altitude difference, figure 4 gives the downshifted plasma lines within the frequency range of from −6.7 to −7.25 MHz at altitudes of 198.52 km, 201.45 km, 204.39 km, 207.32 km, 210.25 km and 339.48 km respectively. In a similar way to the ion line spectrum, those plasma lines show the similar 'breakdowns', but they occur in the GB and HB.

At the altitude of 339.48 km, no pump induced plasma line is found. At the altitude from 198.52 km to 210.25 km, however, there are two 'layers' of plasma lines, the lower ones of which lie at frequency $f_{\rm HF} - \omega_{\rm ia}$ and is the expected 'decay line' from PDI excited by the pump, where $\omega_{\rm ia}$ is the frequency of ion acoustic wave and ∼9.5 kHz here. The most surprising is the upper 'layer' of plasma lines, which show a frequency shifting up of ∼–0.1 MHz from pump frequency and a frequency spread of ∼0.35 MHz, and occur in the HHB and is aligning temporally with those enhancements in P over a wide altitude range. An up-shifting plasma line displaced by about 20 kHz was also seen in EISCAT very high frequency observation, which can in no way be explained by PDI [21]. DuBois *et al* [22–24] have developed a scenario where many

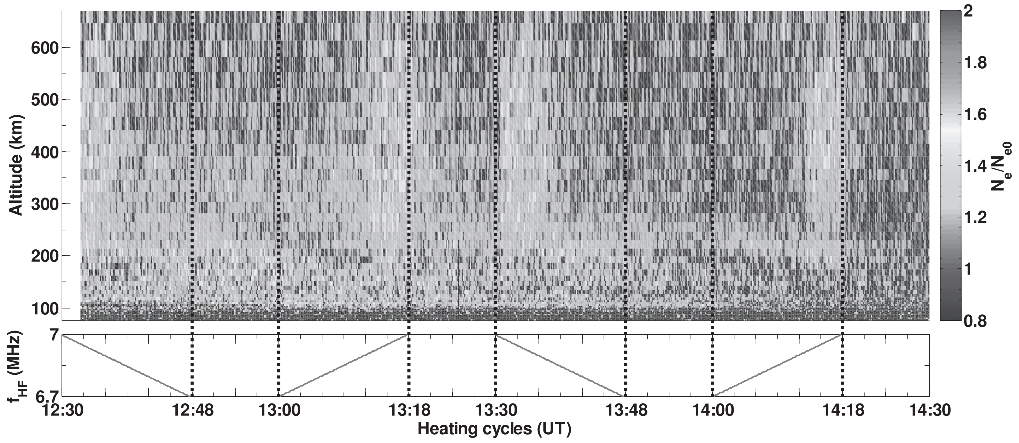

Figure 5. The ratios of N_e to N_{e0} versus heating cycles.

small scale irregularities filled up the heated region and resulted in the up-shifting plasma line. Numerical simulations exhibited a displaced line, whose frequency was larger than the heater frequency, as has been observed at Arecibo and occasionally also at Tromsø site of EISCAT [21–24]. Detailed comparisons with the models provided by DuBois *et al* [22–24] should be done in the future.

3.3. Electron density

Figure 5 is an altitude profile of the ratios of electron density N_e to the undisturbed values of N_{e0} as a function of heating cycle, where N_{e0} denotes the values of the background ionosphere and is taken from the median of the profile of electron density of the final 5 min observations of the last cycle.

In the narrow region around the reflection altitude, it can be seen that there are some enhancements in N_e/N_{e0} during heating in the GB and HB, which should be due to PDI and OTSI shown in figures 3 and 4. In the three wave interaction, the pump (ω_0, $\mathbf{k}_0$) causes the growth of two weak waves (ω_1, $\mathbf{k}_l$) and (ω_2, $\mathbf{k}_2$), where the frequency ω and wave number $\mathbf{k}$ satisfy the matching conditions $\omega_0 = \omega_1 + \omega_2$ and $\mathbf{k}_0 = \mathbf{k}_l + \mathbf{k}_2$, where $\mathbf{k}_0 \approx 0$ can be assumed in ionospheric heating. With regard to PDI, (ω_0, $\mathbf{k}_0$), (ω_1, $\mathbf{k}_l$) and (ω_2, $\mathbf{k}_2$) are associated with the pump, Langmuir wave and ion acoustic wave, and to OTSI, the pump interacts with a Langmuir wave of equal frequency and an ion acoustic wave which is spatially period but has zero frequency. Considering above matching conditions and the electron density profile of ionosphere, at altitude in the interval [20]

$$z_0 - 0.1H \leqslant z_p < z_0, \tag{2}$$

Langmuir and ion acoustic waves can be generated by PDI and OTSI, where z_0 and H denote same parameters as that in formula (1). Based on the reflection altitude of ~207.4 to ~222.4 km obtained by formula (1), PDI and OTSI should be excited within the altitude range of ~202.4 to ~217.4 km.

In addition, the intensity of the pump has to exceed the thresholds of PDI and OTSI as below [25, 26]

$$E_{tp} = \sqrt{4N_{e0}k_B T_i \nu/(\varepsilon_0 \omega_{pe} B_{max})}, \tag{3}$$

$$E_{to} = \sqrt{\left[4\left(1 + \frac{T_e}{T_i}\right)N_{e0}k_B T_i \nu\right] \Big/ (\varepsilon_0 \omega_{pe})}, \tag{4}$$

to overcome such saturation process as collision, where T_i, ν and k_B are the ion temperature, electron collision frequency and the Boltzmann constant, B_{max} a function of T_e/T_i and with a value of ~0.56 for $T_e/T_i = 2$ [27]. During the experiment focused in this paper, T_i, T_e/T_i and ν at the altitude of 200 km measured by UHF radar are ~1000 K, ~1.95 and ~10 Hz respectively, then one can obtain $E_{tp} \approx 0.036$ V m^{-1} and $E_{to} \approx 0.046$ V m^{-1}. Considering the propagation in free space, for the pump with ERP (kW) $\approx 10^5$ and the altitude of R (km) = 200, the electric field should be $E \approx 0.25\sqrt{\text{ERP}}/R$, namely, ~0.4 V m^{-1} [18, 25]. It is obvious that the thresholds of PDI and OTSI should be satisfied fully by the pump.

Once the threshold has been exceeded by the pump, the natural ion acoustic wave amplitudes are increased and consequently, a larger backscattered power is received by the radar, furthermore, the enhancement in electron density is obtained from ion line spectrum integration according to standard analysis of incoherent scattering spectrum. During the experiment focused in this paper, the ion acoustic wave excited by PDI and OTSI can enhance the power of ion line and travel downward and be seen at those altitudes of 203.7 km, 206.63 km, 209.58 km, 212.51 km, 215.43 km shown in figure 3, where the radar Bragg condition $|\mathbf{k}| = 2\ |\mathbf{k}_r| \approx 39$ m^{-1} is satisfied, where $\mathbf{k}$ and $\mathbf{k}_r$ are wave number of ion acoustic wave and radar wave respectively. Therefor, according to standard analysis of incoherent scattering spectrum, those remarkable enhancements in electron density occurring in the HB and GB around the reflection altitude of the pump appears to be consistent with the behavior of ion line spectrum and does not correspond to the true increase in electron density.

In the HHB, there are some strong enhancements in N_e/N_{e0} up to the order of ~1.8, which extend from approximately the pump wave reflection altitude to ~650 km and are apparently altitude independent. Obviously, those enhancements are in alignment temporally with the enhancement in P/P_0 over a wide altitude range and the frequency shifting of plasma line around the reflection altitude, and can't interpreted by PDI and OTSI. Indeed, it is obvious that those large electron density enhancements over a wide altitude range are not natural, but induced the ionospheric heating. Therefore, there should be some possible ways to be responsible for transporting pump energy upward when heating, one of which is that the pump is coupled to Z mode near the critical angle and propagates upward, and the other of which is a plasma transport process, such as diffusion along the magnetic field due to thermal pressure and density gradients. However, the above two ways failed to explain those large electron density enhancements or large enhancements in radar echo with wide altitude extent in HHB [17]. With exception of transporting pump energy upward in pump wave propagation and plasma transport process, we should also take radar wave into account rather than only the pump. Rietveld *et al* [28] suggested a hypothesis where the field-aligned irregularities are much larger than the radar wavelength, and perhaps with hundreds of meter scale size, and cause the grazing radar waves to be reflected. If the irregularities are extended long enough along the field line, multiple reflections can occur so that the region of irregularities acts as a duct where the overall decrease of the radar's field strength with distance falls off more slowly than r^2, where r is the propagating distance. It is this slower decrease of radar wave with distance than the free-space fall-off as r^2 assumed in the normal incoherent scatter analysis that causes the stronger backscatter from all ranges above the ducting region of irregularities. If the above hypothesis is reasonable, there should be stronger radar backscatter above the ionospheric irregularities, from which an enhancement in electron density can be obtained by the standard analysis of the incoherent scattering spectrum. So far, a question arises, that is, whether the large scale irregularities can focus or collimate the radar wave at the frequency of 930 MHz. Regularly, the ionospheric irregularity should not almost act on the radar wave at 930 MHz. However, it seems to be possible in reference to the scintillation effect of ionospheric irregularities on GPS signal in L band (Rietveld M T, private communication).

Figures 1, 4 and 5 show the temporal synchronization of those enhancements in radar backscatter and those enhancements in electron density over a wide altitude range as well as the frequency shifting and spread of plasma lines around the reflection altitude of the pump, which seems to imply that the above synchronization is due to same physical mechanism. Those unstructured frequency spread of plasma line are in frequency range of ~−6.9 to ~−7.25 MHz, which correspond to electron densities from $6 \times 10^{11}\,\mathrm{m}^{-3}$ to $6.5 \times 10^{11}\,\mathrm{m}^{-3}$. So far, two questions rise, namely, (1) whether the irregularities with electron density of $6 \times 10^{11}\,\mathrm{m}^{-3} - 6.5 \times 10^{11}\,\mathrm{m}^{-3}$ can focus or collimate the radar wave at frequency 930 MHz. (2) what mechanism is response for those irregularities? It seems there remains much work to be done in the future.

In figure 5, when heating in the LB in the first cycle, there is a slight decrease in electron density around the reflection altitude, which are coincident temporally with the decreases in P/P_0 and P respectively and should be a result of the trapping of upper hybrid wave excited by the pump at upper hybrid resonance altitude [12]. As is well known, an O mode pump can couple through either pre-existing or artificially induced small scale irregularity into an upper hybrid wave at upper hybrid resonance altitude [29–31], where pump frequency yields

$$f_{\mathrm{HF}} = f_{\mathrm{UH}} = \sqrt{f_{\mathrm{pe}}^2 + \Omega_{\mathrm{ce}}^2}, \quad (5)$$

here f_{UH} denotes the upper hybrid frequency. The upper hybrid wave propagates in a direction perpendicular to the magnetic field and dissipates energy through Ohmic, furthermore, heats electrons, finally, leads to an effect of reducing electron density due to thermal electron transport. Here we assume an individual small scale irregularity with constant initial electron density N_1, whose upper hybrid frequency is $\omega_{\mathrm{UH}}^{N_1}$ and the second cutoff frequency $\omega_{\max}^{N_1}$ [12] (the maximum of Bernstein dispersion curve of the small scale irregularity as a function of wave number, with regard to the experiment reported in this paper, the second cutoff frequency $\omega_{\max}^{N_1}$ should be ~6.848 598 MHz in the first cycle, ~6.826 168 MHz in the second cycle, ~6.842 991 MHz in the third cycle and ~6.834 579 MHz in the fourth cycle), and the background ionospheric plasma N_0 with the upper hybrid frequency $\omega_{\mathrm{UH}}^{N_0}$. Moreover, it is also assumed that the electron density of the small scale irregularity is slightly smaller than that of the background ionospheric plasma, namely, $N_1 < N_0$, that is to say, $\omega_{\mathrm{UH}}^{N_0}$ should be larger than $\omega_{\mathrm{UH}}^{N_1}$. When the pump is operated at a particular frequency between $\omega_{\max}^{N_1}$ and $\omega_{\mathrm{UH}}^{N_1}$, namely, in the LB, the upper hybrid wave with a smaller wave number in N_0 excited by the pump can propagates into the small scale irregularity N_1 and be trapped, furthermore, dissipates energy through Ohmic and heats electrons in N_1. Thus, due to the escape of thermal electron from N_1, the depth of N_1 increases further. When the pump is operated at a higher frequency being closer to fifth gyrofrequency, namely, $\omega_{\max}^{N_1} < f_{\mathrm{HF}} < 5\Omega_{\mathrm{e}}$, the upper hybrid wave excited by the pump in N_0 is reflected on the surface of N_1 and can't propagate into N_1. Thus, the trapping of upper hybrid waves will not take place in N_1 and N_1 will not grow. Additionally, when the pump sweeps in the HB, namely, slightly above $5\Omega_{\mathrm{e}}$, the Bernstein dispersion curves of N_0 and N_1 do almost coincide, then the trapping of upper hybrid wave should be poor.

It was unfortunate that the similar decrease in electron density can not be seen obviously in the second, third and fourth cycles. This may be due to the lower electron density of background ionosphere in the second, third and fourth cycles than that in the first cycles, and the difficulty to measure the relatively small change in artificial electron density using EISCAT UHF radar, or both. Indeed, the electron density changes induced by powerful pump is difficult to measure for the following reasons. The density is much more variable both in time and space, and the artificial density change is relatively small [31]. So, here we hypothesize reasonably that the slight decrease in electron density around

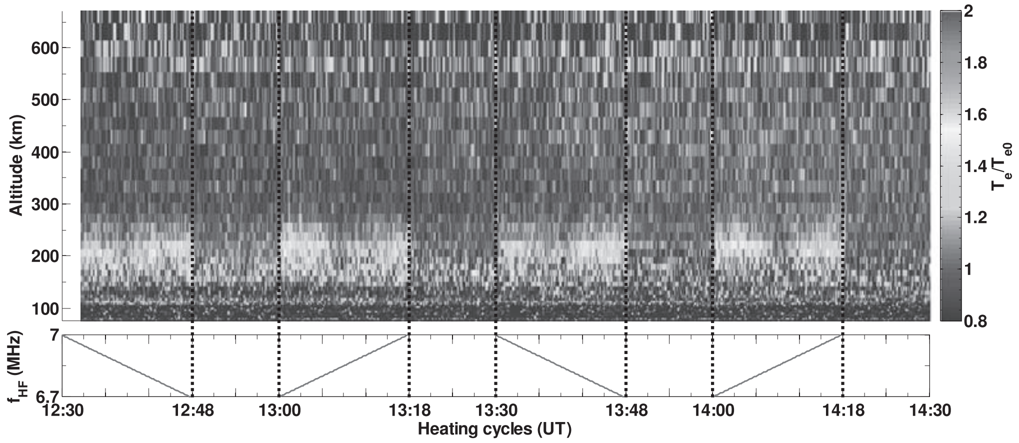

Figure 6. The ratios of T_e to T_{e0} versus heating cycles.

the reflection altitude should have happened in the second, third and fourth cycles, but were not observed by UHF radar due to the above reasons discussed. This hypothesis is important for the following discussion.

3.4. Electron temperature

The altitude profile of the ratios of electron temperature T_e to the undisturbed values of T_{e0} as a function of heating cycle, are provided by figure 6, similarly, where T_{e0} is gave by the median of the profile of electron temperature taken from the final 5 min observations. When heating is on, there is a strong enhancement in T_e/T_{e0} extending around the reflection altitude, which varies with pump frequency f_{HF} in particular and disappears when heating is off. When f_{HF} approaches 6.7 MHz and sweeps in the LB, T_e/T_{e0} enhances strongly up to the order of ~1.6, whereas there is slightly less enhancement in T_e/T_{e0} of approximately up to the order of ~1.4 for f_{HF} in the HB. When f_{HF} is in the GB and very close to $5\Omega_{ce}$, T_e/T_{e0} is approximately on the order of ~1.2 and is less than in both the LB and HB. Consequently, it is noticeable that

$$(T_e/T_{e0})_{LB} > (T_e/T_{e0})_{HB} > (T_e/T_{e0})_{GB}, \quad (6)$$

where $(T_e/T_{e0})_{LB}$, $(T_e/T_{e0})_{HB}$ and $(T_e/T_{e0})_{GB}$ indicate T_e/T_{e0} when the pump operates in the LB, HB and GB respectively.

Based on the hypothesis given in section 3.3 that there should be some slight decreases in electron density around the reflection altitude in the LB, then it is easily understand that the upper hybrid wave excited by the pump can be trapped by the small scale irregularity created by the pump with a growth time 0.5–5 s [32], and dissipates energy sufficiently through the collision damping. As a result, electrons are heated and escape along the magnetic field from N_l, furthermore, the lower cooling rate should be caused by poor thermal coupling between the lower density plasma and the neutral atmosphere in N_l. Thus, the strong enhancement in electron temperature in the LB is not only due to the higher heating rate caused by the trapped upper hybrid wave, but the lower cooling rate caused by the escape of heated electron.

When $f_{HF} \geqslant 5\Omega_e$, however, the upper hybrid dispersion curve of N_0 coincides almost with the Bernstein dispersion of N_l for the small wave number. In this situation, the trapped upper hybrid wave by N_l should propagate in phase velocity $\omega_{UH}^{HB}/k_{UH}^{HB}$, where ω_{UH}^{HB} and k_{UH}^{HB} denote the frequency and wave number of the trapped upper hybrid wave in the HB respectively. Due to $\omega_{UH}^{HB} > \omega_{UH}^{LB}$ and $k_{UH}^{HB} < k_{UH}^{LB}$, where ω_{UH}^{LB} and k_{UH}^{LB} are the frequency and the wave number of the trapped upper hybrid wave in the LB respectively, we can obtain $\omega_{UH}^{HB}/k_{UH}^{HB} > \omega_{UH}^{LB}/k_{UH}^{LB}$, which means the absorption of the trapped upper hybrid by N_l through the collision damping in the HB may be poorer than that in LB, then $(T_e/T_{e0})_{HB} < (T_e/T_{e0})_{LB}$.

In the GB, due to the absence of the trapping of upper hybrid waves, N_l do not grow. It is the absence of the trapping of upper hybrid wave to result in the lowest heating rate at upper hybrid resonance altitude in the GB, namely, $(T_e/T_{e0})_{HB} > (T_e/T_{e0})_{GB}$.

4. Summary and conclusions

This paper reports experimental observation of electron density and electron temperature enhancement for pumping near the fifth electron gyrofrequency on 11 March 2014 at EISCAT. Those irregularities induced by the pump may insult in the focusing or collimating of radar wave and furthermore lead to the stronger radar echo, from which the enhancement in electron density can be deduced through the standard analysis of incoherent scatter. Some additional strong enhancements in electron density occurring around the reflection altitude are not the true increase in electron density, but due to the enhancements in ion acoustic wave excited by PDI and OTSI.

In addition, due to the higher heating rate and the lower cooling rate, the strongest enhancement occurs below the fifth electron gyrofrequency. The second strongest occurring above the fifth electron gyrofrequency is due to the lower heating rate, whereas those enhancements in electron temperature at pump frequency very close to the fifth electron gyrofrequency are much less than that both below and above the fifth electron gyrofrequency, due to the absence of the trapping of upper hybrid wave excited by the pump.

Acknowledgments

We would like to thank the staff of EISCAT in Tromsø for keeping the facility in excellent working condition and Tromsø Geophysical Observatory, UiT The Arctic University of Norway, for providing the magnetic data of Tromsø recorded on 11 March 2014. The EISCAT Scientific Association is supported by China (China Research Institute of Radiowave Propagation), Finland (Suomen Akatemia of Finland), Japan (the National Institute of Polar Research of Japan), Norway (Norges Forkningsrad of Norway), Sweden (the Swedish Research Council) and the UK (the Particle Physics and Astronomy Research Council of the United Kingdom). This work is supported by NSFC (No. 40831062).

References

[1] Gordon W E, Showen R and Carlson H C Jr 1971 *J. Geophys. Res.* **76** 7808
[2] Gordon W E and Carlson H C Jr 1974 *Radio Sci.* **9** 1041
[3] Newman A L *et al* 1988 *Geophys. Res. Lett.* **15** 311
[4] Duncan L M, Sheerin J P and Behnke R A 1988 *Phys. Rev. Lett.* **61** 239
[5] Stocker A J *et al* 1992 *J. Atmos. Terr. Phys.* **54** 1555
[6] Utlaut W F and Violette E J 1974 *Radio Sci.* **9** 895
[7] Mantas G P, Carlson H C Jr and LaHoz C H 1981 *J. Geophys. Res.* **86** 561
[8] Robinson T R *et al* 1996 *J. Atmos. Terr. Phys.* **58** 385
[9] Gurevich A V, Lukyanov A V and Zybin K P 1995 *Phys. Lett.* A **206** 247
[10] Gurevich A V, Lukyanov A V and Zybin K P 1996 *Phys. Lett.* A **211** 363
[11] Gurevich A V *et al* 1999 *Phys. Lett.* A **251** 311
[12] Mjølhus E 1993 *J. Atmos. Terr. Phys.* **55** 907
[13] Honary F *et al* 1995 *J. Geophys. Res.* **100** 21489
[14] Ponomarenko P V, Leyser T B and Thidé B 1999 *J. Geophys. Res.* **104** 10081
[15] Borisova T D *et al* 2014 *Radiophys. Quantum Electron.* **57** 1
[16] Borisova T D *et al* 2016 *Radiophys. Quantum Electron.* **58** 561
[17] Wu J, Wu J and Xu Z W 2016 *Plasma Sci. Technol.* **18** 890
[18] Rietveld M T *et al* 1993 *J. Atmos. Terr. Phys.* **55** 577
[19] Rishbeth H and van Eyken A P 1993 *J. Atmos. Terr. Phys.* **55** 525
[20] Stubbe P, Kohl H and Rietveld M T 1992 *J. Geophys. Res.* **97** 6285
[21] Kohl H *et al* 1993 *J. Atmos. Terr. Phys.* **55** 601
[22] DuBois D F, Rose H A and Russell D 1988 *Phys. Rev. Lett.* **61** 2209
[23] DuBois D F, Rose H A and Russell D 1990 *J. Geophys. Res.* **95** 21221
[24] DuBois D F, Rose H A and Russell D 1991 *Phys. Rev. Lett.* **66** 1970
[25] Robinson T R 1989 *Phys. Rep.* **179** 79
[26] Bryers C J *et al* 2013 *J. Geophys. Res. Space Phys.* **118** 7472
[27] Stubbe P *et al* 1984 *J. Geophys. Res. Space Phys.* **89** 7523
[28] Rietveld M T and Senior A 2015 Do ionospheric irregularities focus UHF radar waves? *17th Int. EISCAT Symp. (Hermanus, RSA, 14–18 September)*
[29] Dysthe K B *et al* 1982 *Phys. Scr.* **1982** 548
[30] Mjølhus E 1990 *Radio Sci.* **25** 1321
[31] Rietveld M T *et al* 2003 *J. Geophys. Res.* **108** 1141
[32] Gurevich A V 2007 *Phys.—Usp.* **50** 1091